First-harmonic diffusion-based model applied to a polyvinyl-alcohol–acrylamide-based photopolymer

Cristian Neipp

Departamento de Física, Ingeniería de Sistemas y Teoría de la Señal, Universidad de Alicante, Apartado 99, E-03080 Alicante, Spain

Sergi Gallego and Manuel Ortuño

Departamento Interuniversitario de Óptica, Universidad de Alicante, Apartado 99, E-03080 Alicante, Spain

Andrés Márquez, Mariela L. Alvarez, and Augusto Beléndez

Departamento de Física, Ingeniería de Sistemas y Teoría de la Señal, Universidad de Alicante, Apartado 99, E-03080 Alicante, Spain

Inmaculada Pascual

Departamento Interuniversitario de Óptica, Universidad de Alicante, Apartado 99, E-03080 Alicante, Spain

Received September 19, 2002; revised manuscript received April 17, 2003

The photopolymerization diffusion models give accurate comprehension of the mechanism of hologram formation inside photopolymer materials. Although several models have been proposed, these models share the common assumption that there is an interplay between the processes of monomer polymerization and monomer diffusion. Nevertheless, most of the studies to check the validity of the theoretical models have been done by using photopolymers of the DuPont™ type, or photopolymer materials with values of the monomer diffusion time similar to those of the DuPont material. We check the applicability of a modified diffusion-based model to a polyvinyl alcohol–acrylamide photopolymer. This material has the property of longer diffusion times for the monomer to travel from the unexposed to the exposed zones than in the case of other polymeric materials. Some interesting effects are observed and theoretically treated by using the modified first-harmonic diffusion-based model we propose.

OCIS codes: 090.0090, 090.7330, 090.2900, 160.5470.

1. INTRODUCTION

Photopolymers are systems of organic molecules that rely on photoinitiated polymerization to record volume-phase holograms. Characteristics such as good light sensitivity, large dynamic range, good optical properties and relatively low cost make photopolymers one of the most promising materials for write-once–read-many (WORM) holographic data storage applications.[1]

Photopolymer systems for recording holograms typically comprise one or more monomers, a photoinitiation system, and an inactive component often referred to as a binder.[2] Other components are sometimes added to control a variety of properties such as sensitivity and viscosity of the recording medium. The mechanism of hologram formation is assumed to be a consequence of the interplay between the processes of monomer polymerization and monomer diffusion that take place when the material is illuminated.[3] These processes are taken into account in all diffusion-based models of the mechanisms of hologram formation.[3–10]

As a result of the availability of commercial polymers such as DuPont™ photopolymer, much work has been done in understanding the dynamics of grating formation in polymer materials. For instance, Zhao and Moroulis[3] studied experimentally the holographic recording process in DuPont dry photopolymer. They proposed a theoretical model that comprises the basic ideas of all diffusion-based models. That is, as a result of the exposure to light, the monomers initially present in the binder are polymerized. If the material is exposed to an interference pattern of light, a gradient of monomer concentration is created inside the material. Then diffusion of monomer from the nonexposed zones to the exposed zones occurs. The variation of monomer concentration with time is then a consequence of two mechanisms: monomer diffusion and monomer polymerization. This model was later refined by Colvin *et al.*[4] and used by them to predict the temporal evolution of the diffraction efficiency for volume gratings recorded in a polymeric medium containing photopolymerizable acrylate monomers. In the model proposed by Zhao and Mourolis,[3] the refractive index was assumed to depend linearly on the polymer concentration. Because the refractive indices of the monomer and polymer are different, Aubrecht *et al.*[5] stated that the first or-

0740-3224/2003/102052-09$15.00

der of the refractive index depends linearly on the first order of the polymer concentration, but also on the first order of the monomer concentration. Kwon *et al.*[6] also considered the influence of the first order of the monomer concentration on the refractive index modulation and studied experimentally a DuPont photopolymer, finding good agreement between the theoretical model and their experimental data. Another complete model was proposed by Sheridan *et al.*,[7] Lawrence *et al.*,[8] and O'Neill *et al.*,[9] which they called a "nonlocal response diffusion model." This nonlocal response of the material is due to the growth of the chains of photopolymer away from their initiation point, which implies a spreading of the photopolymer.

On the other hand Piazolla and Jenkins[10] developed a first-harmonic diffusion model by considering only the first order of the refractive index and the monomer concentration. This model had the advantage that an analytical expression of the refractive-index modulation was obtained that permitted a simple interpretation of the process dynamics. In their model Piazolla and Jenkins assumed that the rate of variation of the refractive index is proportional to the rate of diffusion of the free monomer. This assumption was based in turn on the supposition that photopolymerization does not change locally the refractive-index modulation, and this is related to the local variation of material mass density. Nonetheless, the refractive indices of the polymer and monomer are different, thus not only is material mass density important, but the particular polymer and monomer concentrations play an important role in the mechanism of hologram formation.[5] To introduce this hypothesis we propose a new first-harmonic diffusion-based model. We also compare in this work the theoretical results with experimental data obtained for volume transmission–diffraction gratings recorded in a polyvinyl alcohol (PVA)–acrylamide photopolymer. Because the polymer studied presents a high thickness, overmodulation effects are also described. We stress the significance of the hypothesis we have added to the previous model of Piazolla and Jenkins. We will see that some features of the refractive-index-modulation-versus-time curves can be explained when applying our modified model.

2. THEORETICAL MODEL

A. First Harmonic Diffusion-Based Model

We will first assume that the material is exposed to a sinusoidal interference pattern of the form

$$I(x) = I_0[1 + m\cos(K_g x)], \tag{1}$$

where m is the beam intensity modulation, K_g the grating wave number, and I_0 the average recording intensity.

Because the conversion of monomer to polymer is more rapid in the bright regions than in the dark ones, we will assume that the free monomer presents a sinusoidal spatial concentration which is phase shifted 180° with respect to the intensity pattern. Therefore, the concentration of monomer $\phi^{(m)}$ can be expressed as

$$\phi^{(m)}(x, t) = \phi_0^{(m)}(t) - \phi_1^{(m)}(t)\cos(K_g x). \tag{2}$$

On the other hand, in the bright regions the monomer is converted into polymer. Therefore the polymer concentration $\phi^{(p)}$ takes the form

$$\phi^{(p)}(x, t) = \phi_0^{(p)}(t) + \phi_1^{(p)}(t)\cos(K_g x). \tag{3}$$

As the result of polymerization the concentration of monomer decreases with time. Simultaneously, as the result of the gradient of monomer concentration established between the nonexposed and exposed zones, the free monomer diffuses from the dark to the bright regions. Equation (4) describes the variation of monomer concentration taking into account these two processes.

$$\frac{\partial \phi^{(m)}}{\partial t} = -k_R(t) I^{\delta}(x) \phi^{(m)}(x, t) + \frac{\partial}{\partial x} D \frac{\partial}{\partial x} \phi^{(m)}(x, t), \tag{4}$$

where ϕ stands for the volume fractions of the different compounds; (m) and (p) stand for monomer and polymer, respectively; D is the diffusion constant, which we assume to be constant; I is the illumination intensity, δ is the reaction rate constant, and $k_R(t)$ is the polymerization rate. Equation (4) retains the form of equation proposed by Piazolla and Jenkins[10] to describe the consumption of free monomer. We also introduce Eq. (5), which describes the increase of polymer concentration due to polymerization:

$$\frac{\partial \phi^{(p)}}{\partial t} = k_R(t) I^{\delta}(x) \phi^{(m)}(x, t). \tag{5}$$

Equations (3) and (5) were not considered in Piazolla and Jenkins's model since they stated that the refractive index change was dependent only on the variation in monomer concentration. Nonetheless, the refractive indices of the polymer and monomer are different,[5] thus the polymer concentration must be considered in order to obtain the refractive-index modulation created in the material. An interesting approximation of the dynamics of hologram formation taking into account the differing refractive indices of the polymer and monomer was made by Aubrecht *et al.*[5] According to their mathematical treatment the refractive index of the material n composed of polymer, monomer, and binder can be related to the refractive indices of the individual components by using

$$\frac{n^2 - 1}{n^2 + 2} = \phi^{(m)}\left(\frac{n_m{}^2 - 1}{n_m{}^2 + 2} - \frac{n_b{}^2 - 1}{n_b{}^2 + 2}\right) + \phi^{(p)}\left(\frac{n_p{}^2 - 1}{n_p{}^2 + 2} - \frac{n_b{}^2 - 1}{n_b{}^2 + 2}\right) + \frac{n_b{}^2 - 1}{n_b{}^2 + 2}, \tag{6}$$

where n_p, n_m, and n_b are the refractive indices of the polymer, monomer, and binder, respectively.

Aubrecht *et al.*[5] studied grating formation by investigating the temporal variation of the individual harmonic components of the spatial distribution of the refractive index. An infinite set of coupled equations was then obtained. In their approach it is difficult to obtain quantitative information on the different parameters of the theoretical model by fitting experimental data of the temporal evolution of the diffraction efficiency. In our analy-

sis we will retain only the first harmonic of the refractive index, as was done by Piazolla and Jenkins.[10]

The first-harmonic component of the refractive index can be expressed as[5]

$$n_1 = C_1[-C_2\phi_1^{(m)} + C_3\phi_1^{(p)}], \tag{7}$$

where

$$C_1 = \frac{(n_{\mathrm{dark}}{}^2 + 2)^2}{3n_{\mathrm{dark}}}, \tag{8}$$

$$C_2 = \left(\frac{n_m{}^2 - 1}{n_m{}^2 + 2} - \frac{n_b{}^2 - 1}{n_b{}^2 + 2}\right), \tag{9}$$

$$C_3 = \left(\frac{n_p{}^2 - 1}{n_p{}^2 + 2} - \frac{n_b{}^2 - 1}{n_b{}^2 + 2}\right), \tag{10}$$

and where n_{dark} is the refractive index of the mixture of compounds without illumination. By using Eqs. (1)–(3), Eqs. (4) and (5) can be converted into

$$\frac{\partial}{\partial t}\phi^{(m)}(x, t) = -k_R(t)I_0^{\delta}[1 + m\delta\cos(K_g x)] \times [\phi_0^{(m)} - \phi_1^{(m)}\cos(K_g x)] + \frac{\phi_1^{(m)}}{\tau_D}\cos(K_g x), \tag{11}$$

$$\frac{\partial}{\partial t}\phi^{(p)}(x, t) = k_R(t)I_0^{\delta}[1 + m\delta\cos(K_g x)] \times [\phi_0^{(m)} - \phi_1^{(m)}\cos(K_g x)], \tag{12}$$

where the following approximation was made[10]: $I(x)^{\delta} \approx I_0^{\delta}[1 + m\delta\cos(K_g x)]$. This approximation turns out to be exact for $\delta = 1$, which is in fact the value of the rate constant used in our theoretical fits.

The diffusion time constant τ_D is defined as $\tau_D = 1/DK_g{}^2$.

Finally, the following expressions for the harmonic terms can be derived:

$$\frac{\mathrm{d}\phi_0^{(m)}}{\mathrm{d}t} = -k_R(t)I_0^{\delta}\left(\phi_0^{(m)} - \frac{m\delta}{2}\phi_1^{(m)}\right), \tag{13}$$

$$\frac{\mathrm{d}\phi_1^{(m)}}{\mathrm{d}t} = k_R(t)I_0^{\delta}(m\delta\phi_0^{(m)} - \phi_1^{(m)}) - \frac{\phi_1^{(m)}}{\tau_D}, \tag{14}$$

$$\frac{\mathrm{d}\phi_0^{(p)}}{\mathrm{d}t} = k_R(t)I_0^{\delta}\left(\phi_0^{(m)} - \frac{m\delta}{2}\phi_1^{(m)}\right), \tag{15}$$

$$\frac{\mathrm{d}\phi_1^{(p)}}{\mathrm{d}t} = k_R(t)I_0^{\delta}(m\delta\phi_0^{(m)} - \phi_1^{(m)}). \tag{16}$$

Equations (13)–(16) combined with Eq. (7) are the basic equations of this first-harmonic diffusion model.

B. Analytical Solution for Constant Polymerization Rate

First we will derive an analytical solution of Eqs. (13)–(16) for the case of constant polymerization rate, $k_R(t) = k_0$. By doing this, the main aspects of the theoretical model can be understood.

To solve Eqs. (13)–(16) we assume that before exposure there is only monomer, equally distributed in the material with concentration ϕ_0. Therefore

$$\phi_1^{(m)}(0) = \phi_0^{(p)}(0) = \phi_1^{(p)}(0) = 0, \tag{17}$$

and

$$\phi_0^{(m)}(0) = \phi_0. \tag{18}$$

Provided that the polymerization rate is constant, the solutions of Eqs. (13)–(16) are

$$\phi_0^{(m)}(t) = \frac{\phi_0}{\alpha}\exp\left[-\left(\frac{\gamma}{m\delta} + \frac{1}{2\tau_D}\right)t\right] \times \left[\sinh\left(\frac{\alpha}{2\tau_D}t\right) + \alpha\cosh\left(\frac{\alpha}{2\tau_D}t\right)\right], \tag{19}$$

$$\phi_1^{(m)}(t) = \frac{2\phi_0\gamma\tau_D}{\alpha}\exp\left[-\left(\frac{\gamma}{m\delta} + \frac{1}{2\tau_D}\right)t\right]\sinh\left(\frac{\alpha}{2\tau_D}t\right), \tag{20}$$

$$\phi_0^{(p)}(t) = \phi_0\left[1 - \frac{\phi_0^{(m)}(t)}{\phi_0}\right], \tag{21}$$

$$\phi_1^{(p)}(t) = \frac{2\phi_0}{[-2 + I_0^{\delta}k_0(-2 + m^2\delta^2)\tau_D]} \times \left\{\frac{1}{\alpha}\exp\left[-\left(\frac{\gamma}{m\delta} + \frac{1}{2\tau_D}\right)t\right] \times \left[\left(m\delta - \frac{2\gamma^2\tau_D^2}{m\delta} + \gamma^2\tau_D^2 m\delta\right) \times \sinh\left(\frac{\alpha}{2\tau_D}t\right) + m\delta\alpha\cosh\left(\frac{\alpha}{2\tau_D}t\right)\right] - m\delta\right\}, \tag{22}$$

where

$$\alpha = \sqrt{1 + 2\gamma^2\tau_D^2}, \tag{23}$$

and

$$\gamma = I_0^{\delta}k_0 m\delta. \tag{24}$$

To comprehend the basic ideas of the model we will make two further assumptions that allow us to obtain a simpler closed form of the first order of the refractive index:

$$\delta = m = 1. \tag{25}$$

Setting $\delta = 1$ means that the polymerization rate is proportional to the interference pattern, which is in fact the assumption made in most of the diffusion-based models,[3–5] whereas the value of $m = 1$ was taken for simplicity.

By using Eqs. (20), (22), and (7) the first harmonic of the refractive index can be obtained. The first order of the refractive index has the form

$$n_1 = \frac{2C_1\phi_0}{(2 + \gamma\tau_D)}\left(\frac{1}{\alpha}\exp\left[-\left(\gamma + \frac{1}{2\tau_D}\right)t\right] \times \left\{[(C_3 - C_2)\gamma^2\tau_D^2 - 2C_2\gamma\tau_D - C_3] \times \sinh\left(\frac{\alpha}{2\tau_D}t\right) - C_3\alpha\cosh\left(\frac{\alpha}{2\tau_D}t\right)\right\} + C_3\right), \tag{26}$$

where the value of γ under the assumptions of Eq. (25) is now

$$\gamma = I_0 k_0 . \tag{27}$$

Figure 1 depicts the general form of the first harmonic of the refractive index as a function of time. One can see that the amplitude of the grating modulation increases with time until a maximum value of $n_{1\mathrm{sat}}$. From Eq. (26) the value of the maximum achievable modulation is

$$n_{1\mathrm{sat}} = \frac{2C_1C_3\phi_0}{(2 + \gamma\tau_D)}, \tag{28}$$

which is proportional to C_1, C_3, and to the initial concentration of monomer ϕ_0.

Some aspects of expressions (26) and (28) will be discussed in order to outline the dynamics of the mechanism of hologram formation. First, we want to comment on the proportionality of $n_{1\mathrm{sat}}$ with respect to C_3 as given by Eq. (10). A simple calculation gives

$$C_3 = 3\left(\frac{1}{{n_b}^2 + 2} - \frac{1}{{n_p}^2 + 2}\right). \tag{29}$$

From Eq. (29) it can be seen that C_3 increases with the difference between the refractive index of the polymer and the refractive index of the binder $(n_p - n_b)$ with a consequent increase of the value of $n_{1\mathrm{sat}}$ [Eq. (28)]. This can be easily understood if we remember that for long times of exposure, all the monomer has been converted into polymer. Therefore, in the bright regions the material is composed of polymer and binder whereas in the dark ones there is only binder; no monomer remains in the material. The refractive index modulation is, then, a consequence of the differences in refractive index between these zones, which in turn depends on the refractive indices of the polymer and binder only.

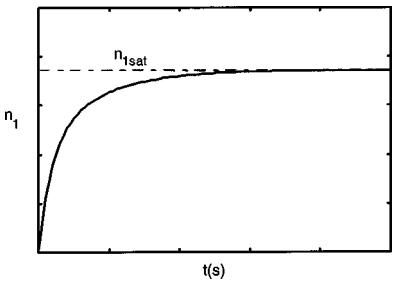

Fig. 1. General form of the first order of the refractive index as a function of time.

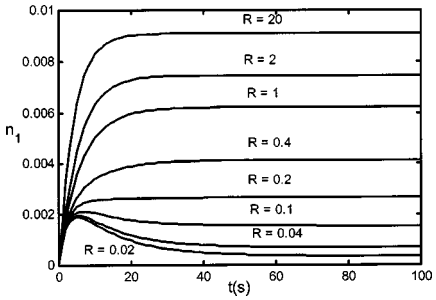

Fig. 2. First order of the refractive index as a function of time for different values of R. The following values were considered: $I_0 = 10\ \mathrm{mW\,cm^{-2}}$; $k_0 = 0.025\ \mathrm{cm^2\,mW^{-1}\,s^{-1}}$.

The dependence of $n_{1\mathrm{sat}}$ on the product $\gamma\tau_D$ also needs comment. To make a comparison with the models of Refs. 3–6 we will change the form of Eq. (28):

$$n_{1\mathrm{sat}} = \frac{2C_1C_3\phi_0}{(2 + 1/R)}, \tag{30}$$

where R is defined as

$$R = \tau_p/\tau_D . \tag{31}$$

With the polymerization time τ_p defined as

$$\tau_p = 1/\gamma, \tag{32}$$

then

$$\tau_p = 1/I_0k_0 \quad \text{for} \quad \delta = m = 1. \tag{33}$$

As can be seen from Eq. (30) the value of $n_{1\mathrm{sat}}$ grows as R increases, which is the same behavior as that described in Refs. 3–5. The analytical expression of the refractive-index modulation of Eq. (30) has the advantage that the behavior discussed can be directly checked. An interpretation of this behavior was provided by Aubrecht *et al.*[5] If we want to attain high values of $n_{1\mathrm{sat}}$, the diffusion time τ_D must be lower than the polymerization time τ_p in order that the monomer not become polymerized before it reaches the interference maximum; this in turn requires $R \gg 1$. Figure 2 shows the first order of the refractive index as a function of time for different values of R given by Eq. (30). In general, the curves show the same tendency as those of Refs. 3–5: the higher the value of R, the higher the maximum and steady-state values of the first order of the refractive index as a function of time. Nevertheless, curves corresponding to R values of 0.1, 0.04 and 0.02 better resemble curves shown by Kwon *et al.*[6] for these low values of R. These curves for values of $R \ll 1$ present first a peak followed by a decrease of the refractive-index modulation. In this case $\tau_D \gg \tau_p$; thus most of the monomer is consumed before it can reach the exposed zones, and the modulation of polymer concentration $\phi_1^{(p)}$ decreases. It is important to stress that it is for values of $R \ll 1$ where differences between our model and those of Refs. 3, 4 and 7–10 arise. This is because expression (7) becomes a relation of proportionality of n_1 with the first order of polymer concentration, as assumed in the models in Refs. 3, 4, and 7–9, when the first order of monomer concentration is negligible. This occurs[5]

when most of the monomer is already converted to polymer, which is the case for long values of the exposure time or when $\tau_p \gg \tau_D\,(R \gg 1)$.

To help understand better the dynamics of polymerization and diffusion, Figs. 3(a) and 3(b) are presented. The first orders of the monomer and polymer concentration, both normalized to the initial monomer concentration, are presented as a function of the diffusion time τ_D and the time of exposure t. The value of the exposure intensity is $I_0 = 5\ \mathrm{mW\,cm^{-2}}$ and $k_0 = 0.015\ \mathrm{cm^2\,mW^{-1}\,s^{-1}}$. The behavior of the first harmonic of the monomer concentration [Fig. 3(a)] is the same as that shown by Piazolla and Jenkins.[10] The curves of $\phi_1^{(m)}$ as a function of time have a fast-rising peak followed by a decrease. We can see that the rate of growth of $\phi_1^{(m)}$ is controlled by the exponential factor in Eq. (19): For a fixed value of γ, increasing values of τ_D imply slower growth of the first harmonic of monomer concentration. Figure 3(b) shows the first harmonic of the polymer concentration as a function of the diffusion time and the time of exposure. Two families of curves can be observed: For low values of the diffusion time $\tau_D\,(R \gg 1)$, the first harmonic of the polymer concentration rises monotonically to a saturation value, whereas for high values of the diffusion times $(R \ll 1)$ the curves of $\phi_1^{(p)}$ as a function of time exhibit a first peak followed by a decrease. This behavior is consonant with the comments made on the influence of R on the first order of the refractive index: For $R \gg 1$ the monomers are polymerized in the bright regions, whereas for $R \ll 1$ the monomers are consumed before they reach the exposed zones.

Another notable aspect of Eq. (26) is that the rate of growth of the first harmonic of the refractive index is controlled by the exponential through the diffusion time τ_D and the polymerization time τ_p. The higher the values of τ_D and τ_p, the slower the rate of growth of n_1 as a function of time. This explains the fact that for high values of the intensity, low values of τ_p result (see Eq. 33) and the saturation refractive-index modulation $n_{1\mathrm{sat}}$ is reached earlier. This is a well-known feature exhibited by experi-

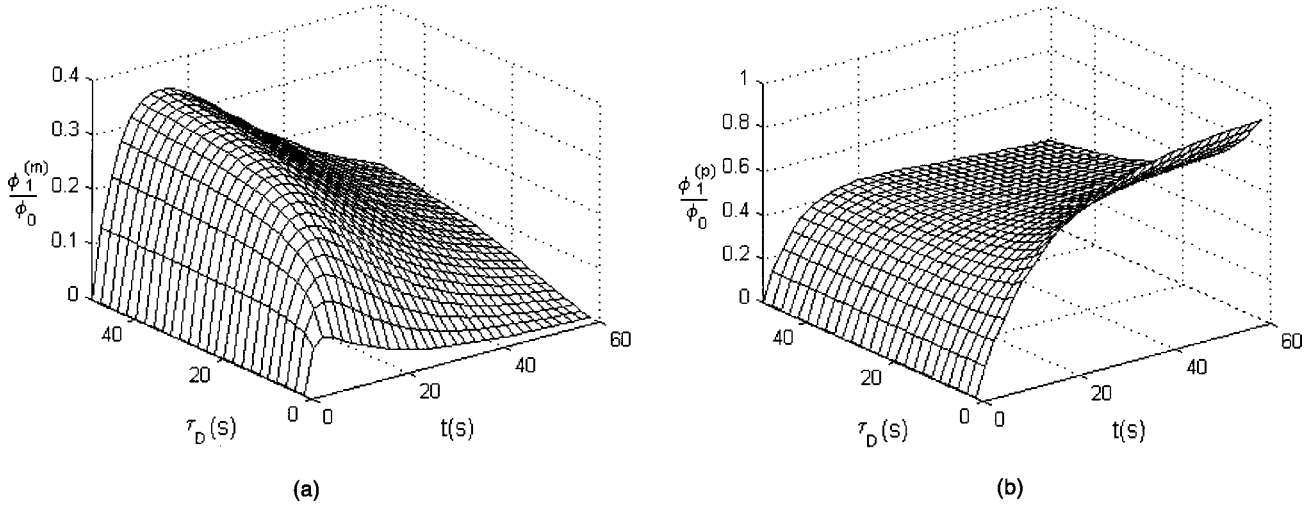

Fig. 3. First order of (a) the monomer and (b) the polymer concentration normalized to the initial monomer concentration as a function of the time of exposure for different values of the diffusion time. The following values were considered: $I_0 = 5\ \mathrm{mW\,cm^{-2}}$; $k_0 = 0.015\ \mathrm{cm^2\,mW^{-1}\,s^{-1}}$.

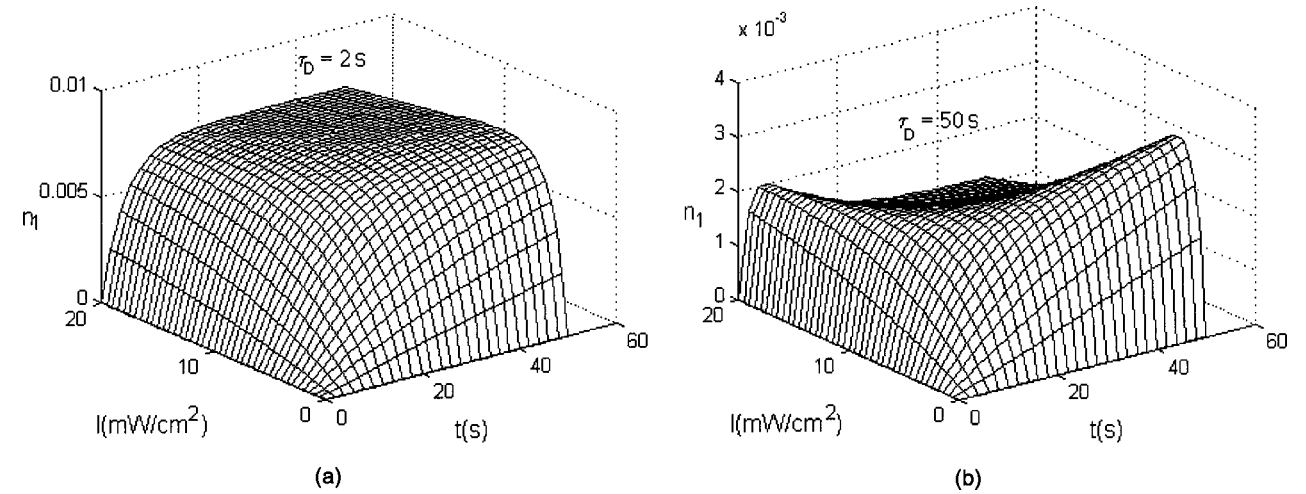

Fig. 4. First order of the refractive index as a function of the time of exposure for different values of the average recording intensity. The following values were considered: $\phi_0 = 0.06$; $k_0 = 0.015\ \mathrm{cm^2\,mW^{-1}\,s^{-1}}$; $\tau_D =$ (a) 2 s, (b) 50 s.

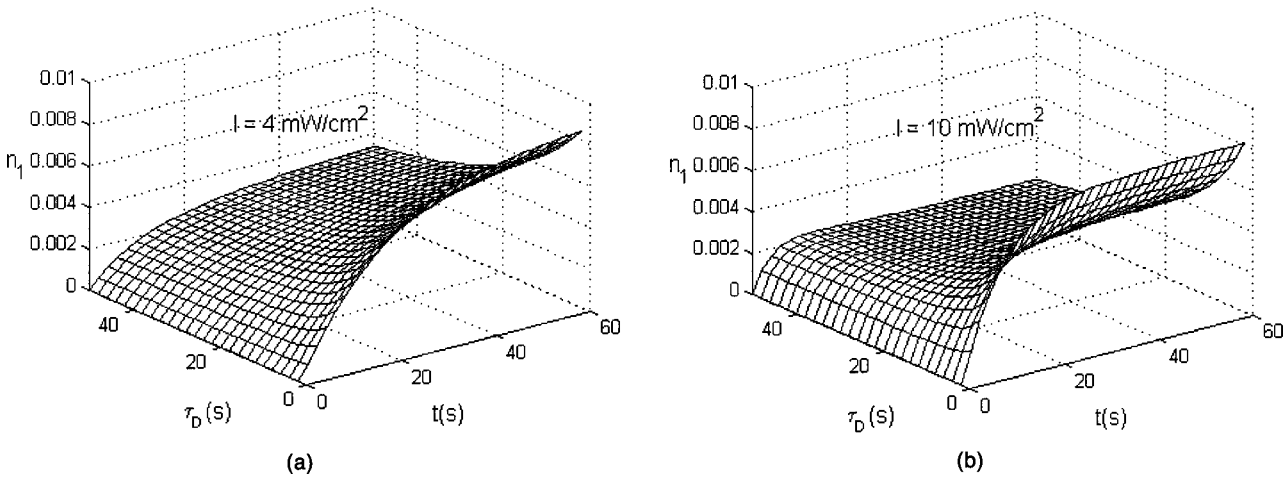

Fig. 5. First order of the refractive index as a function of the time of exposure for different values of the diffusion time. The following values were considered: $\phi_0 = 0.06$, $k_0 = 0.015\,\mathrm{cm^2\,mW^{-1}\,s^{-1}}$; $I_0 =$ (a) $4\,\mathrm{mW\,cm^{-2}}$, (b) $10\,\mathrm{mW\,cm^{-2}}$.

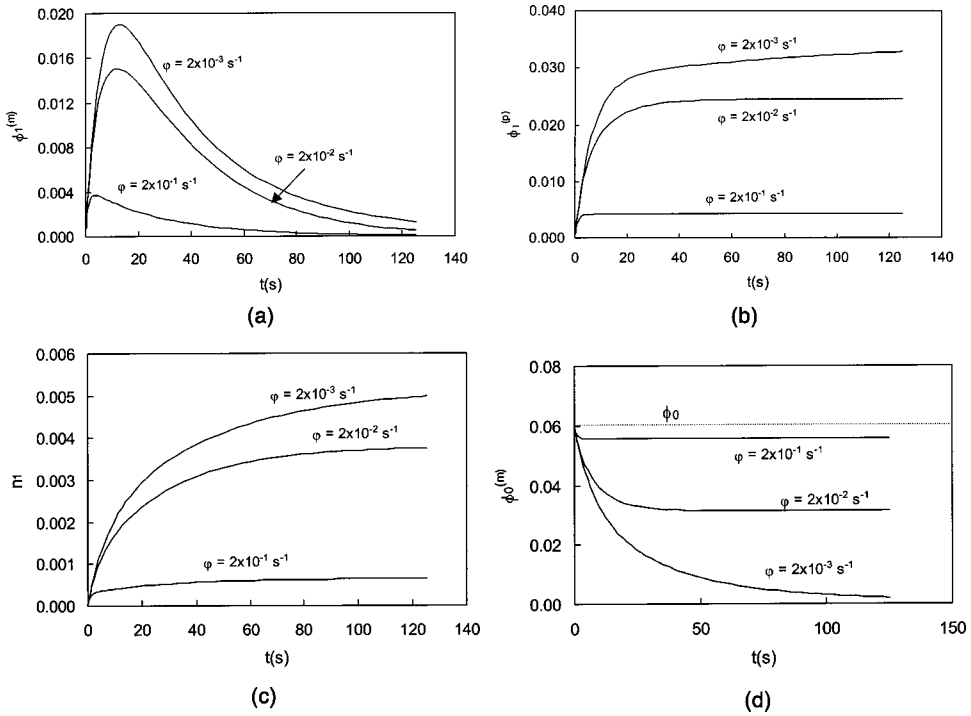

Fig. 6. First order of (a) monomer concentration, (b) polymer concentration, (c) refractive index, and (d) average monomer concentration as a function of the time of exposure for different values of φ. The following values were considered: $I_0 = 5\,\mathrm{mW\,cm^{-2}}$, $k_0 = 0.015\,\mathrm{cm^2\,mW^{-1}\,s^{-1}}$, $\tau_D = 30\,\mathrm{s}$.

mental curves of the refractive-index modulation as a function of time, and it is also described in Refs. 3–6 and 10. Figures 4(a) and 4(b) show n_1 as a function of time and the average exposure intensity I_0 for two different values of diffusion time, 2 s and 50 s, where the behavior just discussed can be observed. It can be seen that as the average exposure intensity increases, so does the rate of growth of n_1 with time. In Fig. 4(a) it can be seen that with an increase in I_0, the steady states are reached earlier. On the other hand it is interesting to observe the behavior of n_1 with time for a high value of the diffusion time in Fig. 4(b). In this case, when I_0 is sufficiently high, $R \ll 1$ and the curves of n_1 as a function of time first present peaks followed by a decrease with time; this was pointed out when Fig. 2 was discussed. On the other hand Figs. 5(a) and 5(b) show n_1 as a function of time and diffusion time for two different values of exposure intensity, $4\,\mathrm{mW\,cm^{-2}}$ and $10\,\mathrm{mW\,cm^{-2}}$. Again the diffusion time τ_D influences the rate of growth of n_1 with time, and for higher values of τ_D the steady-state values are reached earlier.

C. Numerical Results for a Time-Dependent Polymerization Rate

The results presented in Subsection 2.B represent the cases where the value of the polymerization rate remains constant with time. Nonetheless, experimental

observation[11] demonstrates that this value changes during the polymerization process. Piazolla and Jenkins,[10] for instance, assumed that the polymerization rate increases exponentially with time. They found this dependence on the basis of empirical arguments. Although including a time-varying polymerization rate does not change considerably the physical interpretation of the model presented, its influence needs to be considered.

First we tried to fit the experimental data of the diffraction efficiency as a function of time for our PVA–acrylamide-based photopolymer by assuming a polymerization-rate constant that increases with time. However, we found that the model is more predictable if a decaying polymerization constant is considered. In addition, our experimental observation confirmed that when the recording process finishes there is still free monomer. This can be understood if the polymerization rate is assumed to decrease with time. By taking into account these facts we will assume the following dependence of the polymerization rate constant:

$$k_R(t) = k_0 \exp(-\varphi t). \tag{34}$$

Figures 6(a), 6(b), and 6(c), respectively, show the dependence with time of the first harmonic of monomer and polymer concentrations and the first harmonic of refractive index. When φ increases, on the one hand the saturation values decrease and on the other hand the rate of change of all magnitudes increases. Finally, the effect on the average monomer concentration can be seen in Fig. 6(d), where, as mentioned, it can be observed that the average monomer concentration is nonzero after exposure if a decay of the polymerization rate with time is assumed. The influence of this remaining monomer on the predictions of the model analyzed in Subsection 2.B is basically to lower the saturation refractive-index modulation $n_{1\mathrm{sat}}$. This is due to the fact that at high values of the time of exposure not only is the material composed of polymer and binder in the bright regions and only binder in the dark ones, as mentioned in Subsection 2.B, but it also contains free monomer that remains in the material, so the refractive-index modulation is lowered.

It is also interesting to note that PVA–acrylamide photopolymer systems such as the one used in this work usually contain a cross-linker. Including a cross-linker in the polymer network will increase the rate of polymerization, thus increasing the rate of growth of the refractive-index modulation as a function of time. This can be understood if one takes into account that the addition of a cross-linking monomer supposes a quick rise of polymer molecular weight obtained in the bright zones by cross-linking of polyacrylamide chains, thus increasing the polymerization rate.

3. EXPERIMENTAL RESULTS AND VALIDATION OF THE MODEL

To test the model, transmission diffraction gratings were recorded on a polymeric material. The photopolymerizable solution was prepared, under red light, by adding yellowish eosin together with a solution of acrylamide and triethanolamine to a PVA solution. The concentration of each of the components is listed in Table 1. The resulting solution was deposited on a 20 cm × 40 cm glass plate using an automatic depositor and adjusting the thickness of the film. The plate was dried for a period of 72 h in the dark and under normal laboratory conditions (T = 21–23 °C, HR = 40–60%). Once dried, the plate was cut it into pieces measuring 6.5 cm × 6.5 cm to be used in our experimental setup.

The setup used in the experiments to record the transmission diffraction gratings on the photopolymer is shown in Fig. 7. An argon laser at a wavelength of 514 nm was used to store diffraction gratings by means of continuous laser exposure. The laser beam was split into two secondary beams with an intensity ratio of 1:1, that is $m = 1$. The diameter of these beams was increased to 1 cm with an expander, while spatial filtering was ensured. The object and reference beams were recombined at the sample at an angle of 16.8° to the normal with an appropriate set of mirrors, and the spatial frequency obtained was 1125 lines/mm. The diffracted and transmitted intensity were monitored in real time with a He-Ne laser positioned at Bragg's angle and tuned to 633 nm, at which wavelength the material does not polymerize.

To obtain the diffraction efficiency as a function of the angle at reconstruction, we placed the plates on a rotating stage. Diffraction was calculated as the ratio of the diffracted beam to the incident power; to take into account Fresnel losses, the expression was multiplied by an appropriate factor. The relation between the first-harmonic component of the refractive index n_1 and the diffraction efficiency η for volume-phase holograms in which a sinusoidal diffraction grating has been recorded is given by the following equation[12]:

$$\eta = \exp(-\alpha d/\cos\theta')\sin^2\left(\frac{\pi n_1 d}{\lambda \cos\theta'}\right), \tag{35}$$

Table 1. Composition of Polymeric Material

Component	100 μm
Acrylamide (AA)	0.44 M
Triethanolamine (TEA)	0.20 M
Yellowish eosin (YE)	2.5×10^{-4} M
Dimethyl acrylamide (DMMA)	0.16 M
Polyvinyl alcohol (PVA)	6% w/v

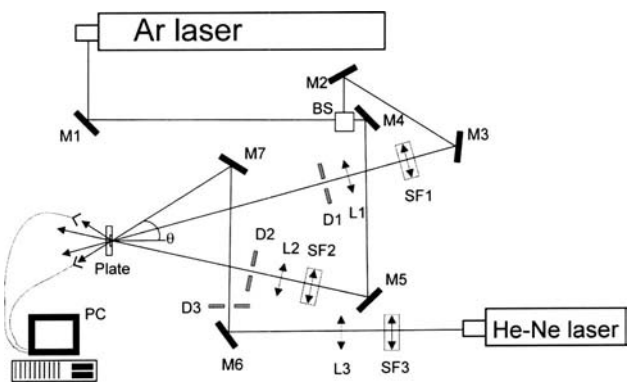

Fig. 7. Experimental setup.

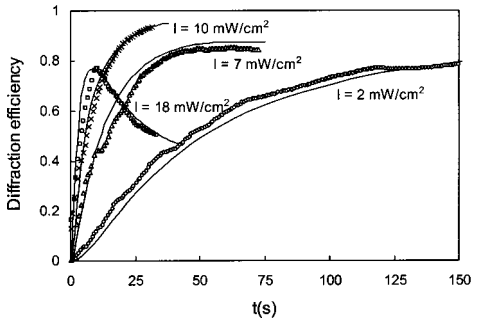

Fig. 8. Diffraction efficiency as a function of time for transmission diffraction gratings recorded on PVA–acrylamide photopolymer at four different intensities. The refractive indices considered were $n_m = 1.56$, $n_b = 1.52$, $n_p = 1.60$.

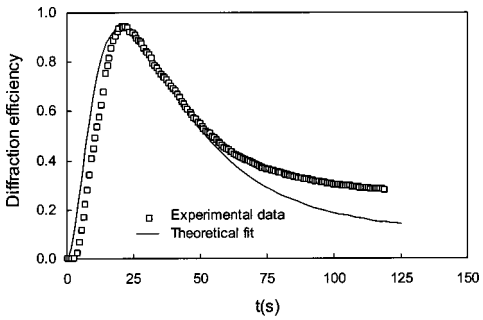

Fig. 9. Diffraction efficienc as a function of time for an overmodulated transmission diffraction grating recorded on a PVA–acrylamide photopolymer. The following values were considered: $I_0 = 2\ \mathrm{mW\,cm^{-2}}$, $k_0 = 0.027\ \mathrm{cm^2\,mW^{-1}\,s^{-1}}$, $\tau_D = 30\ \mathrm{s}$. The refractive indices considered were $n_m = 1.56$, $n_b = 1.52$, $n_p = 1.60$.

where λ is the wavelength of reconstruction in air, α takes into account the absorption and scattering of the hologram (we have no means of differentiating them), d is the thickness of the hologram, and θ' is the angle of reconstruction in the recording medium, related to the angle of reconstruction in air by Snell's law.

Figure 8 shows the diffraction efficiency as a function of time for holographic, unslanted diffraction gratings recorded in PVA–acrylamide photopolymer for different recording intensities. The theoretical curves were obtained by using expression (7). Although we observed slight changes of the polymerization rate constant for the different plates prepared, the value of k_0 was kept in the interval 0.013–0.016 $\mathrm{cm^2\,mW^{-1}\,s^{-1}}$. On the other hand the values of the diffusion time τ_D between 40 and 60 s, high if compared with the typical values of diffusion times used in photopolymers of DuPont type,[10] ~2 s, and φ was found to be in the interval 0.0005–0.0009 $\mathrm{s^{-1}}$. It can be seen in Fig. 8 that the recording intensity is a parameter that controls the rate of increase of the refractive-index modulation, in agreement with other diffusion-based models. As the recording intensity increases, so also does the rate of increase of the refractive-index modulation. This fact is also well described by our theoretical model, and good agreement between the theoretical fits and the experimental data can be seen. On the other hand the high values of the diffusion time allow us to see the behavior of the diffraction efficiency as a function of time for a low value of the parameter R, defined in Subsection 2.B. In the case of the curve that corresponds to the exposure intensity of 18 $\mathrm{mW\,cm^{-2}}$, the parameters of the theoretical fit were as follows: $k_p = 0.015\ \mathrm{cm^2\,mW^{-1}\,s^{-1}}$, $\varphi = 0.0009\ \mathrm{s^{-1}}$, and $\tau_D = 48\ \mathrm{s}$. If we calculate R from Eq. (31), we obtain ~0.07 which is $\ll 1$, and the experimental curve behaves as those shown in Fig. 2 for $R < 0.01$.

Figure 9 shows the diffraction efficiency as a function of time for a holographic diffraction grating recorded in PVA–acrylamide photopolymer exhibiting overmodulation. The curve of squares corresponds to the experimental data, whereas the solid curve corresponds to the theoretical fit. This overmodulated diffraction grating was obtained by increasing the concentration of initial monomer with respect to that of Fig. 8. Although the theoretical curve describes the overall behavior exhibited by the experimental results, it deviates slightly from them at high exposure times. This difference is possibly due to a slight decrease of the diffusion rate at high times of exposure. The decrease in the diffraction efficiency after the peak is due to high values of the product $n_1 d$ of the refractive-index modulation and the thickness of the hologram.[12] This is possible because of the high thickness $d \sim 75\ \mu\mathrm{m}$ of the final holograms recorded in our photopolymer material. Another important aspect that must also be commented on is that an increase in the concentration of acrylamide also meant a decrease in the diffusion time—$\tau_D \sim 30\ \mathrm{s}$—and the polymerization rate constant—$k_0 \sim 0.027\ \mathrm{cm^2\,mW^{-1}\,s^{-1}}$—in accordance with Ref. 3.

4. CONCLUSIONS

A first-harmonic-based model is proposed to explain the mechanism of hologram formation in a photopolymer material. By following the approach of the diffusion-based models, we learn that two processes play the main roles in the formation of the diffraction grating: conversion of monomer into polymer by photopolymerization and diffusion of free monomer from the dark to the bright regions. Because the refractive index of the monomer is different from that of the polymer, the first orders of both the polymer and the monomer concentrations play an important role in the dynamics of grating formation. Thus, both contributions must be taken into account, at least for values of $R \ll 1$, as we have demonstrated.

We have shown an exact solution for the first order of the concentrations of polymer and monomer and for the refractive-index modulation, provided the polymerization rate is constant. The analysis of the closed-form solution of the refractive-index modulation permits easy understanding of the processes involved in the mechanism of hologram formation. For instance, it has been shown that the saturation refractive-index modulation $n_{1\mathrm{sat}}$, depends on the refractive index of the polymer and the binder. On the other hand, the dependence of the refractive-index modulation on the parameter R has also been analyzed, revealing differences in the cases $R \ll 1$ and $R \gg 1$.

The experimental results obtained by recording transmission diffraction gratings on a PVA–acrylamide-based photopolymer validated the theoretical model.

With validation of the model, we can use it to predict new behaviors in the dynamics of hologram formation such as the influence of beam modulation, optimization of the material for successive-angle-multiplexing recording, influence of a slanted geometry in the recording setup, and so forth.

ACKNOWLEDGMENT

This work was supported by Ministerio de Ciencia y Tecnología, Comisíon Interministerial de Ciencia y Tecnología (CICYT), Spain, under project MAT2000-1361-C04-04.

Corresponding author C. Neipp may be reached by e-mail to cristian@disc.ua.es.

REFERENCES

1. D. J. Lougnot, "Self-processing photopolymer materials for holographic recording," in *Polymers in Optics: Physics, Chemistry, and Applications*, R. A. Lessard and W. F. Frank, eds., Critical Review Series **CR63** (SPIE, Bellingham, Wash., 1996), pp. 190–213.
2. S. Blaya, L. Carretero, R. F. Madrigal, and A. Fimia, "Photosensitive materials for holographic recording," in *Handbook of Advanced Electronic and Photonic Materials and Devices, Vol. 7*, H. S. Nalma, ed. (Academic, New York, 2000), Chap. T.
3. G. Zhao and P. Mourolis, "Diffusion model of hologram formation in dry photopolymer materials," J. Mod. Opt. **41**, 1929–1939 (1994).
4. V. L. Colvin, R. G. Larson, A. L. Harris, and M. L. Schilling, "Quantitative model of volume hologram formation in photopolymers," J. Appl. Phys. **81**, 5913–5923 (1997).
5. I. Aubrecht, M. Miler, and I. Koudela, "Recording of holographic diffraction gratings in photopolymers: theoretical modeling and real-time monitoring of grating growth," J. Mod. Opt. **45**, 1465–1477 (1998).
6. J. H. Kwon, H. C. Hwang, and K. C. Woo, "Analysis of temporal behavior of beams diffracted by volume gratings formed in photopolymers," J. Opt. Soc. Am. B **16**, 1651–1657 (1999).
7. J. T. Sheridan, M. Downey, and F. T. O'Neill, "Diffusion based model of holographic grating formation in photopolymers: generalized non-local material responses," J. Opt. A, Pure Appl. Opt. **3**, 477–488 (2001).
8. J. R. Lawrence, F. T. O'Neill, and J. T. Sheridan, "Photopolymer holographic recording material parameter estimation using nonlocal diffusion based model," J. Appl. Phys. **90**, 3142–3148 (2001).
9. F. T. O'Neill, J. R. Lawrence, and J. T. Sheridan, "Comparison of holographic photopolymer materials using analytic nonlocal diffusion models," Appl. Opt. **41**, 845–852 (2002).
10. S. Piazolla and B. J. Jenkins, "First-harmonic diffusion model for holographic grating formation in photopolymers," J. Opt. Soc. Am. B **17**, 1147–1157 (2000).
11. C. García, A. Fimia, and I. Pascual, "Holographic behavior of a photopolymer at high thicknesses and high monomer concentrations: mechanism of photopolymerization," Appl. Phys. B **72**, 311–316 (2001).
12. H. Kogelnik, "Coupled wave theory for thick hologram gratings," Bell Syst. Tech. J. **48**, 2909–2947 (1969).